New Electro-Optic Laser Scanners for Small-Sat to Ground Laser Communication Links

Scott R. Davis,* Seth T. Johnson, Scott D. Rommel, and Michael H. Anderson
Vescent Photonics Inc., 4865 E. 41st Ave., Denver CO 80216

Jimmy Chen and Tien-Hsin Chao
Jet Propulsion Laboratory
4800 Oak Grove Drive, Pasadena CA 91109

ABSTRACT

In this paper we present new electro-optic beam steering technology and propose to combine it with optical telecommunication technology, thereby enabling low cost, compact, and rugged free space optical (FSO) communication modules for small-sat applications. Small satellite applications, particularly those characterized as "micro-sats" are often highly constrained by their ability to provide high bandwidth science data to the ground. This will often limit the relevance of even highly capable payloads due to the lack of data availability. FSO modules with unprecedented cost and size, weight, and power (SWaP) advantages will enable multi-access FSO networks to spread across previously inaccessible platforms. An example system would fit within a few cubic inch volume, require less than 1 watt of power and be able to provide ground station tracking (including orbital motion over wide angles and jitter correction) with a 50 to 100 Mbps downlink and *no moving parts*. This is possible, for the first time, because of emergent and unprecedented electro-optic (EO) laser scanners which will replace expensive, heavy, and power-consuming gimbal mechanisms. In this paper we will describe the design, construction, and performance of these new scanners. Specific examples to be discussed include an all electro-optic beamsteer with a 60 degree by 40 degree field of view. We will also present designs for a cube-sat to ground flight demonstration. This development would provide a significant enhancement in capabilities for future NASA and other Government and industry space projects

Keywords: free space optical communications, laser comm., electro-optic laser scanner, non-mechanical scanner, laser scanner, cube-sat, micro-sat

1. INTRODUCTION & OVERVIEW

In this paper we present a design for ultra-low Size, Weight, and Power (SWaP) Micro-Laser Communications (MiLC) modules for high bandwidth (Mbps or even Gbps) data links between miniature satellites (e.g. cube-sats) and ground stations, satellite clusters, and/or airborne assets (see Fig. 1). The need for this is imminent. Emergent data-intensive collection concepts coupled with dramatic reductions in satellite size will necessitate new low SWaP communications capabilities to avoid bottlenecks. To enable these MiLC modules we will utilize new non-mechanical laser scanners that overcome the historically intractable challenge of providing a viable alternative to mechanics. After decades of trying and 10's to 100's of millions of dollars spent on prior attempts the world still lacks an electro-optic (EO) replacement for the ubiquitous gimbaled mirror. The non-mechanical scanners to be utilized here are enabled by an electro-evanescent optical refraction which will provide *continuous scanning* over $60^o \times 15^o$.[1] Improvements to the scanners promise to increase the FOV up to $120^o \times 120^o$.

* Corresponding author. Tel.: 303-296-6766; fax: 303-296-6783.
Email address: davis@vescentphotonics.com

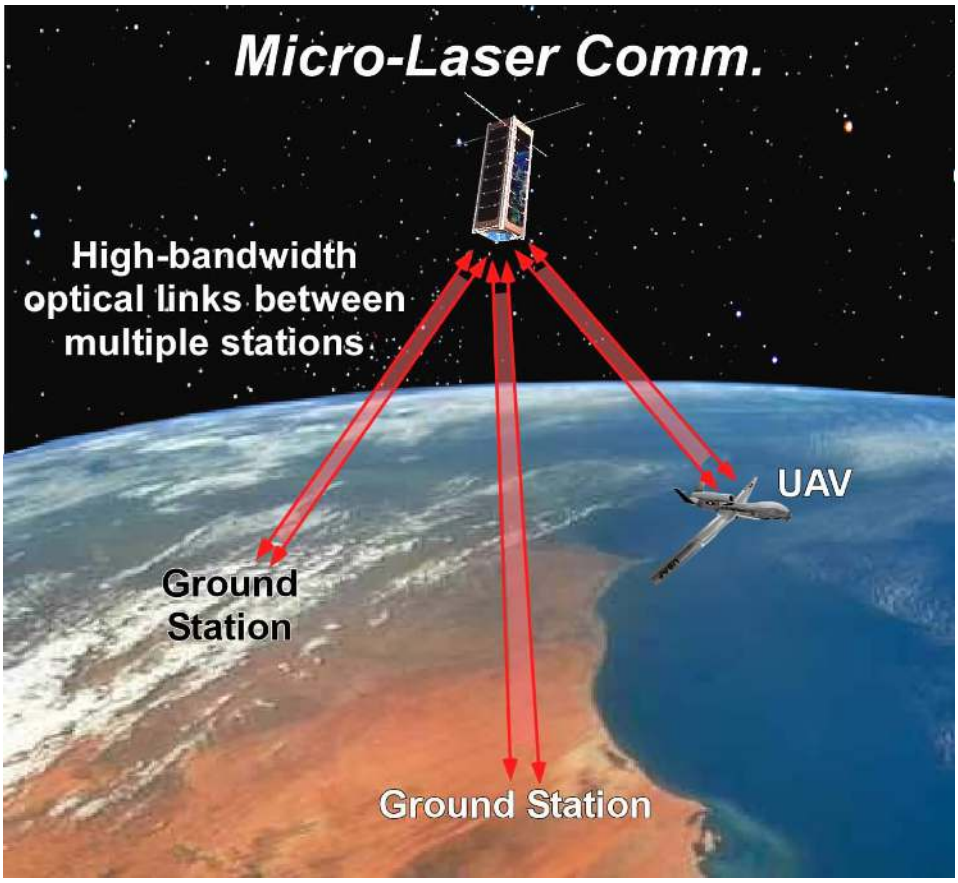

Figure 1: The Micro-Laser Communications (MiLC) concept. These will be enabled by the proposed revolutionary non-mechanical laser scanners.

The advantages to FSO systems are long appreciated, e.g., security, high-bandwidth, lack of RFI, immunity to jamming, and lack of frequency allocation requirements.[2] Unfortunately, the complexity, cost, and SWaP of current mechanically scanned solutions limits their platform applicability. The challenges for cube-sat data-links are an excellent example. We are confident that MiLC systems can meet these challenges. As reported here we have begun a design for a system that could fit within a few cubic inch volume, require less than 1 watt of power and be able to provide ground station tracking (including orbital motion over wide angles and jitter correction) with a >50 Mbps downlink and *no moving parts*. Higher bandwidths are possible with trade-offs.

2. New Electro-Optic Laser Scanners: Circumventing the Size, Weight, and Power Limitations of Mechanics

2.1. Replacing Mechanics: The Long-Standing Dream

EO scanners that provide high-speed, continuous coverage over wide field-of-views (FOVs), extreme pointing accuracy, and are compact and simple have been a long-standing dream of the optical community. Reduced mass and size on spacecraft loading by eliminating traditional gimbals for pointing/tracking allow accommodation of other payloads such as advanced science instruments requiring high bandwidth data capacity. As such, EO replacement for the ubiquitous gimbals would provide new capabilities and enable new missions. Such a reduction in mass and size is particularly relevant and critical for the increasingly utilized low-cost small spacecraft.

Unfortunately, despite both the tremendous desire and the significant amount of resources (four DARPA programs) and time expended viable EO alternatives to mechanics are still not available. Past attempts (e.g., DARPA-STAB, APPLE, etc.) have yielded wide-angle, discrete-step birefringent prisms,[3-5] but these are bulky, expensive, slow, and have wide gaps between scan angles. New polarization grating scanners scanners can realize wide angle in a smaller and less expensive form factor,[6, 7] but these scanners are still "blind" to the vast majority of the field of view. To fill in the gaps between the discrete angles (> 90% of FOV not addressed), prior approaches have utilized tunable diffraction gratings, such as LC optical phased arrays (OPAs),[8-10] MEMs arrays,[11, 12] electro-wetting arrays,[13] and acousto-optics. Despite significant advances, inherent limitations remain. For example, step scanning in OPAs depends on LC relaxation times (typically 5 to 30 ms), so a 500×500 frame would take several hours! Furthermore, OPAs scan in discrete step-wise 2π resets and, therefore, suffer "blind spots" themselves in the FOV into which they cannot steer. While diffractive fine-steering elements have fundamental problems, unfortunately prior *refractive* scanning attempts have realized only small scan angles and/or large beam divergence.[14-19] Until now, this has been a problem without a solution.

2.2. Replacing Mechanics: Finally a Solution

Rather than continue down the well trodden "diffractive-path" we have taken a unique approach to this historically intractable problem. We exploit the giant electro-optic phase control (voltage tuning of optical phase by > 2 mm) provided by proprietary liquid-crystal (LC) clad optical waveguides[20-22] to construct unparalleled *refractive* EO scanners. For near-IR operation (λ~1.5 μm) we have recently demonstrated: i) a 1-D beamsteerer with a remarkable steering range of 270°, ii) wide-angle continuous coverage 2-D beamsteerers ($50^o \times 15^o$ per SEEOR chip) , iii) high speed scanning (60 kHz demonstrated), and iv) a large aperture scanner (1.2 cm demonstrated). These devices are called Steerable Electro-Evanescent Optical Refractors or SEEORS. Figure 2 shows example SEEOR devices which may be extremely compact (~$2cm^3$). They are also inherently low power consumption (only milliWatts) and very simple (only 3-control electrodes for 2-D steering). Finally, the elegance of the design allows for low cost volume production, ultimately similar to the ubiquitous LC-display.

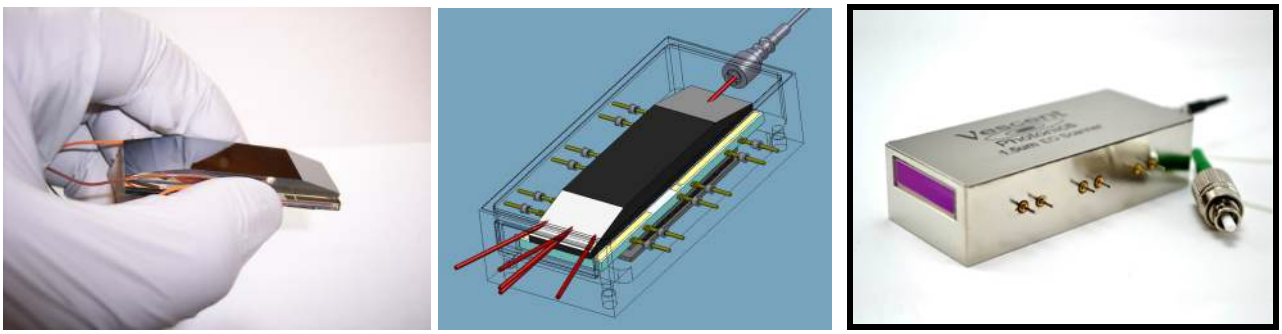

Figure 2: LEFT) The electro-optic waveguide device that provides 2-D EO scanning. A circular, 1550 nm beam enters the device on one of the angled facets and an EO scannable beam exits from the other angled facet. MIDDLE) Solid model of a single chip packaged scanner. RIGHT) Picture of a packaged, fiber coupled 2-D EO scanner.

The enabling innovation for these scanners is to utilize liquid crystals (LCs), which have by far the largest electro-optic response of any known material (R_{33} ~ 10^6 pm/volt compared to ~20 pm/volt for $LiNbO_3$), in a new geometric configuration that circumvents their historic limitations. Rather than transmit through an LC cell, which must be thin (typically < 20 μm) to avoid high scattering losses and slow response times, we utilize the LC as an active cladding layer in a waveguide architecture in which the light is confined to a high index core and the evanescent field extends into the variable-index liquid-crystal cladding (see right of Figure 3). Because the light is confined to the region near the surface where the LC molecules are strongly coupled, they experience strong restoring forces leading to dramatically lower scattering and very fast response times (<500 μsecs). Furthermore, by placing the LC in the evanescent field of the guided optical wave the interaction length is decoupled from the thickness of the LC layer, i.e., *large interaction lengths (up to cm's) are possible with a nicely behaved thin (~5 μm) LC-layer*. This not only circumvents limitations of traditional LC-optics, but it also surpasses the optical phase control performance capabilities of any other EO or MEMs optical system (voltage control over millimeters of optical phase are realized).

Giant voltage control over optical phase enables unprecedented refractive scanning. Horizontal beam steering is achieved by prism shaped electrodes whose index may be voltage tuned (left of Figure 3). Vertical beam steering is achieved by allowing the evanescent field to tunnel into the high-index silicon substrate by tapering the subcladding (right of Figure 3). An S-taper provides a Gaussian output with M^2~1. The output angle $\theta_{vertical}$ may be voltage tuned. For the cube-sat application this will provide 2-D tunable refraction with a $60^o \times 20^o$ FOV and a <2mrad divergent beam. Two of these units placed back-to-back (<8mm thick) preceded by an optical switch will provide a $60^o \times 40^o$ FOV. Figure 4 shows both scan angle data (left) and superimposed frames from a IR-CCD acquired movie wherein a 1550 nm beam was scanned across a parking lot (right). In this example the drive voltage reached 100 volts, but the current draw was negligible (micro-amps); simple DC-to-DC converter circuits are used to realize these voltages in a very small package.

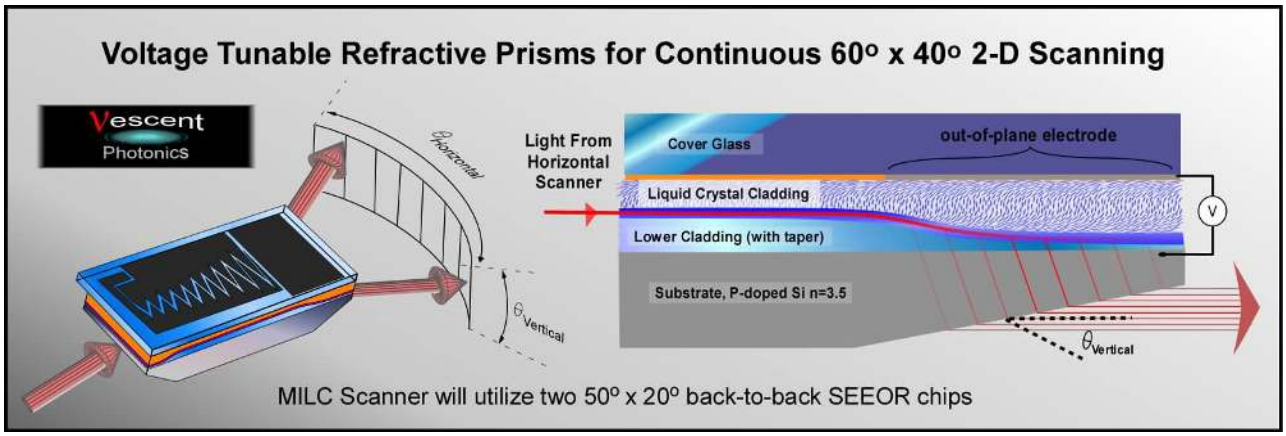

Figure 3: New wide angle, continuous, refractive EO beamsteerers. The light is steered via a voltage tunable Snell's law refraction, either with prism electrodes (horizontal) and/or an out-coupling prism (vertical). The light input and output is a collimated beam.

Since these refractive EO scanners are a new approach this provides some unique advantages over the historical diffractive approaches, including:

- **True Refractive Steering (extreme pointing accuracy):** Since SEEORs are not diffractive (there are no side lobes) efficiency is independent of angular steer range. *Single devices with angular coverage of 180^o or more are possible.* This also provides continuous angular coverage (diffractive optical phased array scanners must step in increments of 2π resets, which limits their pointing precision); SEEOR pointing accuracy is only limited by voltage noise. *Sub micro-radian accuracy is possible*.

- **Continuous Scanning:** Unlike discrete step approaches (such as LC-optical phased arrays), which can miss or step over large angular regions, this approach provides true continuous coverage. There are no blind spots.

- **Rapid Scanning:** The electro-evanescent architecture provides scanning rates across the full FOV from 2 kHz (current scanners) to 10's of kHz (demonstrated a 60 kHz scanner). This enables high frame-rates with complete coverage over the frame.

- **Very Low SWaP:** The simplicity of the approach minimizes SWaP. SEEOR scanners use only milliwatts of electrical power, weigh less than 10 grams, take up less than 10 cm^3 of volume, and don't require multi-stages of small-angle and then large-angle steering elements.

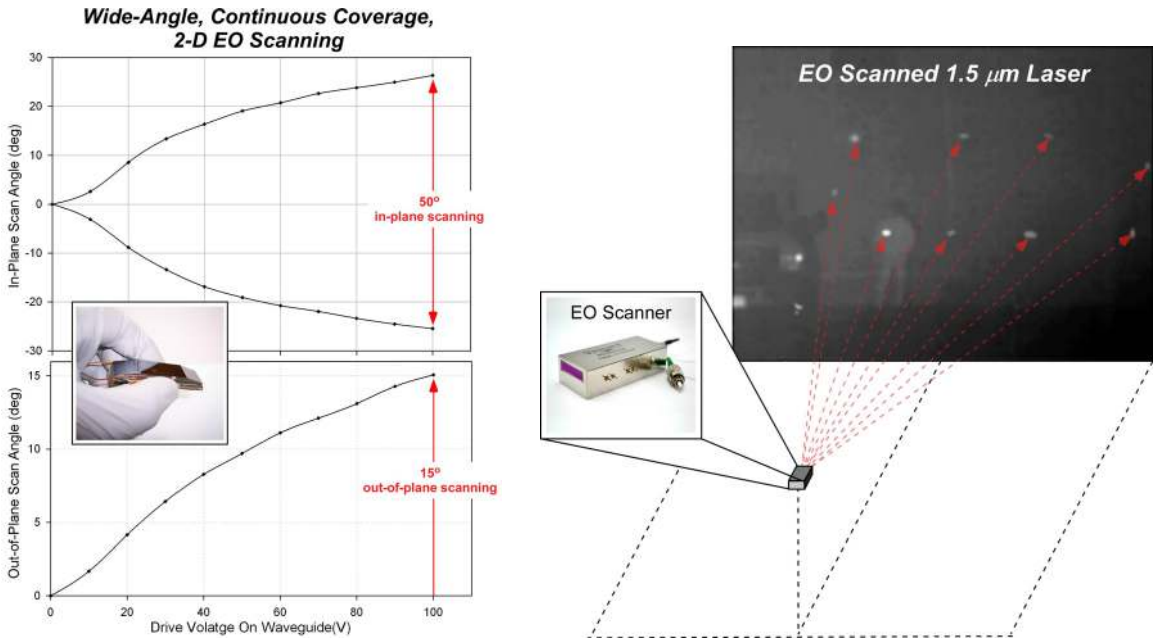

Figure 4: LEFT) Plot of measured EO scan angle as a function of waveguide voltage. The inset picture shows an EO scan waveguide. RIGHT) Superimposed frames from a movie (recorded with an IR InGaAs CCD) showing EO scanning of a 1550 nm laser across a parking lot.

- **High Data Rate:** The single mode optical waveguide geometry is similar to telecom components that have demonstrated >100 Gbit bandwidths. JPL had demonstrated >10 Gbits through SEEORs in an FSO demo.

- **High Resolution:** The ultimate metric for an EO scanner is the number of far-field resolvable spots, or the related Lagrange number. The SEEOR architecture will enable wide aperture (several centimeters possible) and wide angle scanners with *tens of thousands of resolvable spots* (Lagrange numbers > 4 cm ultimately) in a remarkably simple device.

- **Low Cost:** The inherent simplicity of the SEEOR device will enable dramatic cost savings in volume. Ultimately, the devices could be cost comparative to a calculator or watch display.

- **Space Deployable:** In addition to the inherent rugged construction and elimination of all moving parts the LC-waveguide devices are built from materials with demonstrated radiation hardness[23] (> 45 Mrad of Gamma[24] and > 2 Mrad of electron[25]).

3. MiLC INNOVATION AS ENABLED BY NEW SCANNERS

This paper considers combining these new scanners with optical communications technologies to construct Micro-Laser Comm (MiLC) modules. MiLC modules will provide a free space optical (FSO) capability that significantly exceeds existing capability anywhere that we are aware of. Unique advantages to this approach include:

1-**Zero physical disturbance** from the pointing system enables higher system pointing stability and can enable simultaneous data collections and communications.

2- **Multiple downlink points**: KHz bandwidth over continuous coverage wide angles provides the ability to rapidly target alternate ground receivers as an effective mitigation of the most significant FSO objection that is weather-induced blockage. By enabling the system to "instantly" switch between many ground receivers that are hundreds or thousands of km separated, the system will nearly always have access for data downlink.

3-**Jitter compensation** can be provided by the high accuracy, KHz laser beamsteerer. By closing the loop around onboard accelerometers, the system will be capable of stabilizing the downlink beam in the presence of other on-board mechanical disturbances.

This MiLC development is also in alignment with NASA technology roadmaps and addresses NASA technology grand challenges by drastically increasing space communication link capacity at LEO/GEO from current low data rates at RF to high data rates at optical frequencies with low power/mass/size/cost. Space communication technology development must ensure that future space missions of NASA and other agencies are not constrained by a lack of communication capability. The enhanced capacity provided by MiLC will allow future missions to take advantage and to implement new and more capable science instruments that will evolve in the future.

3.1. Laser Communications System Architecture

Figure 2-1 is a potential CubeSat system diagram. The laser link between the space and the ground is bi-directional. The downlink beam is 1550-nm laser beam modulated by payload data for the space data retrieval from ground stations. The SEEOR will keep the downlink beam tracking to the ground station, following the uplink beacon pointing.

Initial acquisition of the Cubesat could be achieved using ephemeris provided by ground tracking. The wide uplink beam would be directed to the satellite to provide the pointing reference from the wide field of view (FOV) acquisition/tracking quadrant detector. The 1000/1 resolution of the acquisition quadrant detector supports milliradian acquisition FOV with microradian resolution. Calibration of the downlink beam pointing relative to the uplink beacon position enables return of the downlink beam to be pointed to the ground receiver.

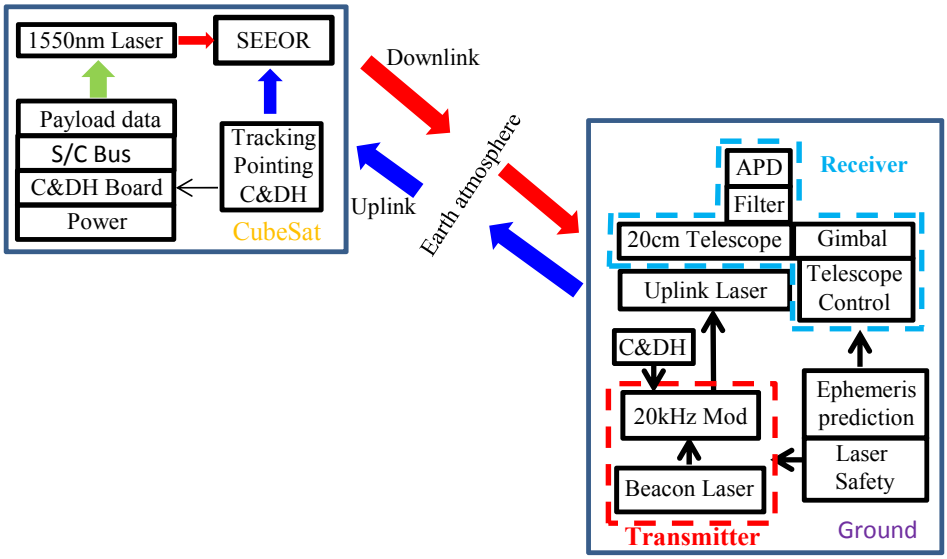

Figure 5: CubeSat system diagram

A portion of the downlink signal captured by the receiver telescope would be directed to an acquisition camera that controls a fast steering mirror to maintain the downlink signal on the avalanche photodiode detector (APD) for the duration of the pass. The wide uplink and downlink beams would avoid the need to implement lead/lag pointing corrections.

3.2. Link Analysis

The MiLC optical link would be initiated by the 10 watts of uplink laser beacon power launched from four 1mm beams (2.5-W/beam) co-aligned with the receiver. The multi-beam uplink mitigates the scintillation effects on the uplink. A 2-kHz modulation impressed on the uplink beacon serves as a reference signal for phase-sensitive detection to suppress the Earth-shine background of daytime operation.

Table 1 is the MILC uplink beacon budget. The 960-nm uplink wavelength is at the peak of the silicon quadrant beacon-tracking detector. For 350-km to 450-km link slant range corresponding to the +/- 30^{o} field of regard of the MILC transmitter the uplink margin ranges from 5.23 dB to 7.41 dB.

The 1-mrad full width half-maximum divergence of the uplink beam design mitigates the effects of expected uncertainty in knowledge of the low Earth orbit (LEO) Cubesat and the demands for high density tracking to generate accurate ephemeris files.

Table 1: Analysis of beacon uplink.

Item	**dB**
Laser power, dBW	10
Transmitter gain, 1mm aperture	70.30
Transmitter losses	-0.97
Path losses	-255.40
Atmospheric zenith transmission	-0.46
Atmospheric loss, 50 deg elevation	-0.60
Receiver gain, 5 cm aperture	104.28
Receiver losses (telescope optics, filter, truncation)	-0.97
Received power, dBW	-73.82
Receiver sensitivity dB(A/W)	-1.43
Detector signal, dBA	-75.25
Quadrant detector loss	-6.02
Dark current, dBA	-86.50
Margin, range 450-km	**5.23**
Margin, range 350-km	***7.41***

Table 2 shows the downlink analysis from the Cubesat. The downlink wavelength is 1550-nm, and the bandwidth of the 200-μm avalanche photodiode detector at the focus of the 20-cm ground receiver readily supports the 50Mb/s on-off-keyed modulation downlink data stream.

The small 20-cm receiver aperture enables link support using a low-cost, high precision tracking gimbal. The aperture gain supports the 50Mb/s downlink from a 1.5-cm sub-aperture through the aperture with 400mW laser power into a 1-mrad beamwidth. Losses in the transmitter and receiver optical trains account for an additional 6 dB of losses in addition to the space loss. On the receiver end the major loss contribution is to the truncation loss at the receiver. The major loss at the transmitter is the SEEOR insertion loss. The link margins range from 7.9-dB at the 450-km slant range at 50 degrees elevation to 10.1-dB at 350-km at zenith.

Table 2: Analysis of Cubesat downlink.

Item	dB
Laser power, dW	-3.98
Transmitter gain	89.66
Transmitter losses	-3.01
Path losses	-249.06
Atmospheric loss	-0.46
Receiver gain, 20 cm	112.16
Receiver losses (telescope optics, filter, truncation)	-3.01
Received power, dBW	-57.70
Receiver sensitivity, dB(A/W)	-0.46
APD signal, dBA	-58.16
Dark current, dBA	-68.24
Margin, 350-km range	**10.10**
Margin, 450-km range	***7.90***

An advantage of the multi-beam wide uplink divergence is the reduced laser intensity propagated through navigable and near-Earth space. The nominal ocular hazard distance of the uplink laser (NOHD) is less than 600-m. The short NOHH reduces the safety threat to the flying public and the expected duration of predictive avoidance outages, should any be imposed by US Space Command's Laser Clearing House.

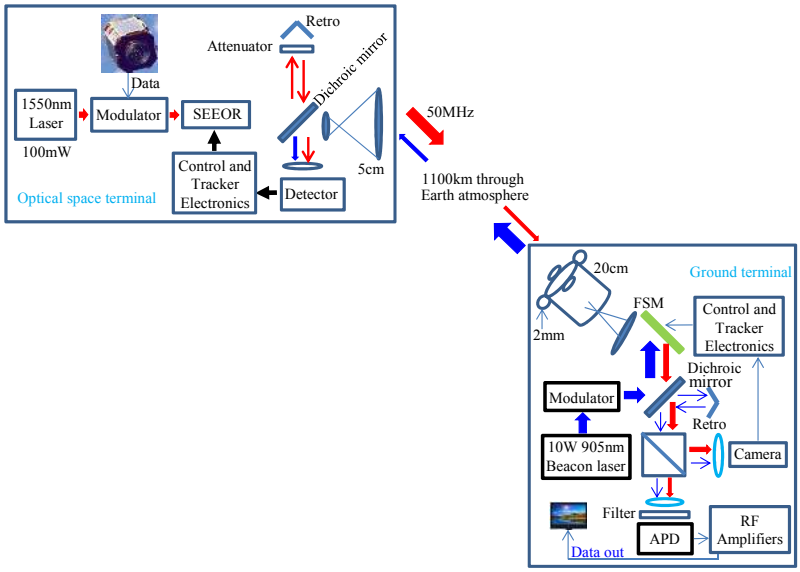

Figure 6: CubeSat system optical terminal link

3.3. Microsat Spacecraft

A first test of this approach is envisioned for a 3U cubesat for the flight demonstration of the SEEOR based laser communications system, as shown in Fig 7. In order to support the proposed technology demonstration, the microsat must have the following capabilities and meet certain Key Requirements as listed below:

- S-Band command and telemetry communications.
- Maintain NADIR point attitude within ±5°.

- Accommodate a 1MP camera with a frame rate of >10 fps, “The Payload”
- Collect and store image data from the payload in a FIFO buffer capable of storing 100 image frames
- Link the spacecraft buffer to the laser comm modulator for wideband data downlink

The cubesat is envisioned as a standard nano-satelite originally developed at Stanford University and California Polytechnic University. MiLC will use a 3U cubesat that measures 10cm x 10cm x 30cm, has approximately a 3 liter volume, and a mass of less than 4kg. There are several possible sources for a cubesat including both commercial off the shelf (COTS) cubesat kits (Pumpkin, Tyvak) as well as universities with cubesat programs (California Polytechnic University San Luis Obispo, University of Michigan).

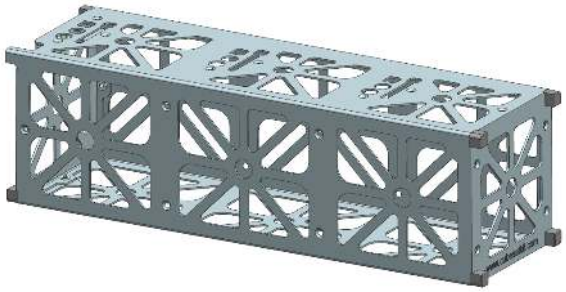

Figure 7: 3U Cubesat Skeletonized Structure

The benefits of using a cubesat are its emphasis on simplicity and low cost. They reduce the complexity and cost of a mission with a standard form factor and compatibility with COTS components.

3.4. Mission Plan and Concept of Operations

One possibility for a test launch would be to use the Poly-Picosatellite Orbital Deployer (P-POD) to interface with/separate from the launch vehicle. The P-POD is a rectangular box designed by Cal Poly with a capacity of 3U worth of cubesats. Its small size allows for easy integration on any launch vehicle. The P-POD will deploy MILC after a signal from the Launch Vehicle. Once separation has occurred, MILC would deploy its solar arrays and point to nadir.

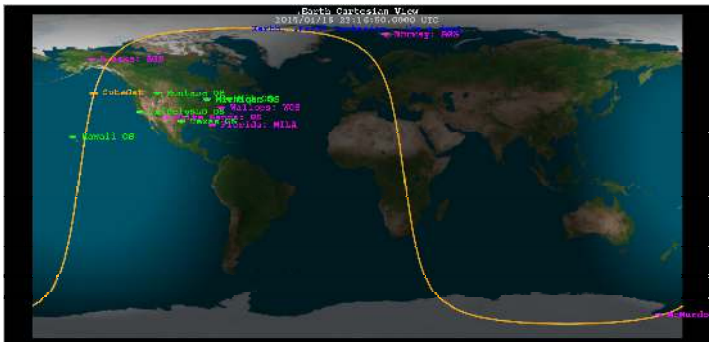

Figure 8: Potential MiLC orbit.

During MILC's first orbit, communications could be established with ground stations at White Sands, Alaska, and/or Wallops via RF downlink. Mission ops would then calculate the orbit ephemeris and orbit propagation and post the information online. This process could be repeated every day to track MILC's orbit throughout the mission. After the initial acquisition, universities around the country would then be able to input the orbit into their laser communication tracking terminal

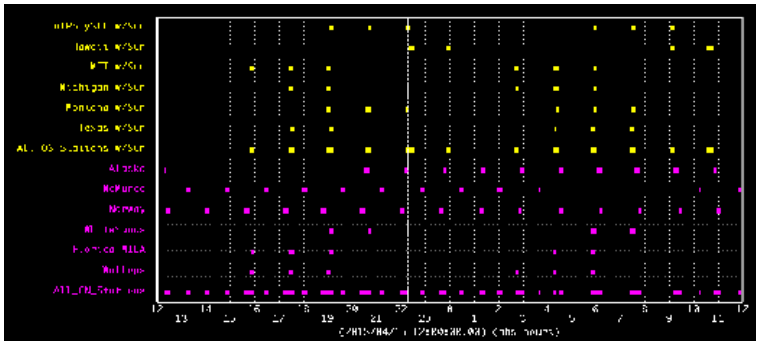

Figure 9: MiLC Optical and Ground Station Coverage

for wideband downlink of data. Figure 8 shows the nominal orbit of MILC as it flies over the optical and ground stations. Figure 9 shows the optical and ground station coverage for a 24 hour period. Table 3 shows the nominal downlink capability in one day using a baseline 600km, circular, sun synchronous orbit and a sample of 6 US universities with cubesat programs.

4. CONCLUSIONS

We have explored the possibility of combining new electro-optic beamsteering technology with optical telecommunication technology to enable compact and rugged free space optical (FSO) communication modules. These FSO modules will have unprecedented size, weight, and power (SWaP) by replacing expensive, heavy and power consumptive mechanics with chip-scale non-mechanical laser scanner. We call our steering technology *steerable electro-evanescent optical refraction* (SEEOR). We believe that it is viable to use *SEEORs* for FSO modules as needed for wide-angle and high angular resolution pointing, acquisition and tracking between satellites, airborne platforms, ground stations, and near Earth spacecraft.

The ultra-compact, low power, and ultimately low cost optical communication systems discussed here have numerous scientific and commercial applications. Commercial applications include last-mile telecommunications environments in urban setting, for field-deployable high-definition video systems for newscasters and sports casters (e.g., high-def coverage of golf tournaments is currently and outstanding challenge), and a variety reconfigurable, low-cost, commercial high-bandwidth data links. Extending the capability to space based platforms will find utility in satellite relay networks, surveillance systems, and general increased communications bandwidths.

Through dramatically higher bandwidth, Terrestrial based optical communications, via fiber-optic-networks, have revolutionized the lives for millions of people. Space based optical communications are poised to play a similar role in space science and exploration. Dramatically higher data rates when compared to existing RF systems (10-100 times faster) will enable the use of bandwidth intensive instruments such as synthetic aperture radar, hyperspectral imagers, and other high definition instruments.

Table 3: MiLC Optical and Ground Station Coverage

Pass #	Pass Start Time (UTC)	Duration (min)	Location	Data Downlink Volume (GB)	# of Images
1	15:45	10.26	MIT	30.78	3847.50
	15:47	8.48	Wallops	-	-
2	17:20	12.75	MIT	38.25	4781.25
	17:21	12.45	Michigan	37.35	4668.75
	17:26	9.40	Texas	28.20	3525.00
	17:22	12.82	Wallops	-	-
3	18:57	0.49	Michigan	1.48	184.64
	18:57	12.05	Montana	36.15	4518.75
	18:57	8.06	MIT	24.18	3022.50
	19:00	12.61	Texas	37.83	4728.75
	19:01	9.84	Cal Poly SLO	29.52	3690.00
	18:59	8.41	Wallops	-	-
	19:00	12.66	White Sands	-	-
4	20:33	12.22	Montana	36.66	4582.50
	20:36	12.65	Cal Poly SLO	37.95	4743.75
	20:40	3.16	Texas	9.48	1185.00
	20:37	9.81	White Sands	-	-
	20:29	10.42	Alaska	-	-
5	22:11	5.61	Montana	16.83	2103.75
	22:14	5.54	Cal Poly SLO	16.62	2077.50
	22:17	12.57	Hawaii	37.71	4713.75
	22:05	12.75	Alaska	-	-
6	23:54	8.91	Hawaii	26.73	3341.25
	23:41	12.65	Alaska	-	-
7	2:39	9.67	MIT	29.01	3626.25
	2:44	2.66	Michigan	7.98	997.50
	2:40	6.31	Wallops	-	-
	2:52	9.39	Alaska	-	-
8	4:13	12.85	MIT	38.55	4818.75
	4:14	12.05	Michigan	36.15	4518.75
	4:17	2.93	Texas	8.79	1098.75
	4:21	3.82	Montana	11.46	1432.50
	4:12	12.66	Wallops	-	-
	4:26	9.24	Alaska	-	-
9	5:47	12.60	Texas	37.80	4725.00
	5:50	12.00	Michigan	36.00	4500.00
	5:51	8.50	MIT	25.50	3187.50
	5:52	7.06	Cal Poly SLO	21.18	2647.50
	5:52	11.91	Montana	35.73	4466.25
	5:49	10.15	Wallops	-	-
	5:48	11.48	White Sands	-	-
	6:00	10.82	Alaska	-	-
10	7:24	9.46	Texas	28.38	3547.50
	7:25	12.77	Cal Poly SLO	38.31	4788.75
	7:27	12.36	Montana	37.08	4635.00
	7:24	11.94	White Sands	-	-
	7:34	12.48	Alaska	-	-
11	9:00	9.22	Hawaii	27.66	3457.50
	9:03	8.89	Cal Poly SLO	26.67	3333.75
	9:09	12.86	Alaska	-	-
12	10:34	12.51	Hawaii	37.53	4691.25
	10:47	10.98	Alaska	-	-

5. ACKNOWLEDGMENTS

This authors wish to thank Keith Wilson and Keith Coste for useful discussions. The electro-optic laser scanner was developed with support from the Navy Research Labs, NASA, and the Air Force Research Laboratories.

6. REFERENCES

[1] S. R. Davis, G. Farca, S. D. Rommel, S. Johnson, and M. Anderson, "Liquid Crystal Waveguides: New Devices Enabled by >1000 Waves of Optical Phase Control," in *Emerging Liquid Crystal Technologies V*, L.-C. Chien, ed. (SPIE, San Francisco CA, 2010), pp. 76180E-76181.

[2] C. C. Davis, I. I. Smolyaninov, and S. D. Milner, "Flexible optical wireless links and networks," IEEE Communications Magazine **41,** 51-57 (2003).

[3] S. A. Kahn, and N. A. Riza, "Demonstration of 3-dimensional wide angle laser beam scanner using liquid crystals," Optics Express **12,** 868-882 (2004).

[4] H. Meyer, D. Riekmann, K. P. Schmidt, U. J. Schmidt, M. Rahlff, E. Schrbder, and W. Thrust, "Design and performance of a 20-stage digital light beam deflector," Applied Optics **11,** 1932-1936 (1972).

[5] Schmidt, and W. Hust, "Optical deflection system including an alternating sequence of birefringent prisms and polarizers," U.S. Patent 3,572,895**,** (1986).

[6] J. Kim, C. Oh, M. J. Escuti, L. Hosting, and S. A. Serati, "Wide-angle, nonmechanical beam steering using thin liquid crystal polarization gratings," in *Advanced Wavefront Control: Methods, Devices, and Applications VI*, (SPIE, 2008), pp. 709302-709301.

[7] S. R. Nersisyan, N. V. Tabiryan, D. M. Steeves, and B. R. Kimball, "The principles of laser beam control with polarization gratings introduced as diffractive waveplates," in *Proc of SPIE* I. C. Khoo, ed. (2010), pp. 77750U-77751.

[8] J. Borel, J.-C. Deutch, G. Labrunie, and J. Robert, "Liquid Crystal Diffraction Grating," U. S. P. Office, ed. (Commissariat A L'Energie Atomique, 1974).

[9] J. P. Huignard, M. Malard, and G. d. Corlieu, "Static Deflector Device for An Infrared Beam," U. S. P. a. T. Office, ed. (Thomson-CSF, USA, 1987).

[10] P. McManamon, P. J. Bos, M. J. Escuti, J. Heikenfeld, S. A. Serati, H. Xie, and E. A. Watson, "A Review of Phased Array Steering for Narrow-Band Electrooptical Systems," Proceedings of the IEEE **97,** 1078-1096 (2009).

[11] R. Ryf, H. R. Stuard, and C. R. Giles, "MEMS tip/tilt & piston mirror arrays as diffractive optical elements," Proceeding of SPIE, Bellingham, WA **5894,** 58940C-58941-58911 (2005).

[12] K. Krishnamoorthy, K. Li, D. Yu, D. Lee, J. P. Heritage, and O. Solgaard, "Dual mode micromirrors for optical phased array applications," Sensors and Actuators A **A97-98,** (2002).

[13] N. R. Smith, D. C. Abeysinghe, J. W. Haus, and J. Heikenfeld, "Agile wide-angle beam steering with electrowetting microprisms," Optics Express **14,** 6557-6563 (2006).

[14] Y. Chiu, R. S. Burton, D. D. Stancil, and T. E. Schlesinger, "Design and Simulation of Waveguide Electrooptic Beam Deflectors," Journal of Lightwave Technology **13,** 2049 (1995).

[15] Y. Chiu, J. Zou, D. D. Stancil, and T. E. Schlesinger, "Shape-Optimized electrooptic beam scanners: Analysis, design, and simulation," Journal of Lightwave Technology **17,** 108 (1999).

[16] J.-h. Kim, L. Sun, C.-h. Jang, C.-C. Choi, and R. T. Chen, "Polymer-based thermo-optic waveguide beam deflector with novel dual folded-thin-strip heating electrodes," Optical Engineering **42,** 620-624 (2003).

[17] D. A. Scrymgeour, Y. Barad, V. Gopalan, K. T. Gahagan, Q. Jia, T. E. Mitchell, and J. M. Robinson, "Large-angle electro-optic laser scanner on LiTaO3 fabricated by in situ monitoring of ferroelectric-domain micropatterning," Applied Optics **40,** 6236 (2001).

[18] J. E. Stockley, S. A. Serati, G. D. Sharp, P. Wang, K. F. Walsh, and K. M. Johnson, "Broadband Beam Steering," in *SPIE Proceedings*, (1997).

[19] K. Nakamura, J. Miyazu, Y. Sasaki, T. Imai, M. Sasaura, and K. Fujiura, "Space-charge-controlled electro-optic effect: Optical beam deflection by electro-optic effect and space-charge-controlled electrical conduction," Journal of Applied Physics **104,** 013105-013101 (2008).

[20] M. Anderson, S. Davis, and S. Rommel, "Liquid Crystal Waveguide having Refractive Shapes for Dynamically Controlling Light," United States Patent # US 8,311,372 B2, 2012

[21] M. Anderson, S. Rommel, and S. Davis, "Liquid Crystal Waveguide having Refractive Shapes for Dynamically Controlling Light," United States Patent # 8,380,025 B2, 2012

[22] S. R. Davis, S. D. Rommel, G. Farca, and M. H. anderson, "A New Electro-Optic Waveguide Architecture and The Unprecedented Devices It Enables," in *SPIE Defense and Security Symposium*, (SPIE, Orlando, FL, 2008), pp. 697503-697501.

[23] E. W. Taylor, "Space and Enhanced Radiation Induced Effects in Key Photonics Technologies. ," in *IEEE Proceedings Aerospace Conference*, (1999).

[24] F. Berghmans, and e. al., "Influence of Gamma Radiation on the Electrooptic Behavior of Planar Nematic Liquid Crystal Cells," IEEE Photonics Technology Letters **9,** 481-483 (1997).

[25] A. Grahm, and e. al., "Preliminary space environment tests of nematic liquid crystals," in *SPIE Photonics for Space Environments IV*, (Denver, CO, USA, 1996).